Acta Cryst. (1995). D**51**, 155–159

Structure of the Ferredoxin from *Clostridium acidurici:* Model at 1.8 Å Resolution

BY D. TRANQUI

Laboratoire de Cristallographie, CNRS, 166X, F38042, Grenoble, France

AND J. C. JÉSIOR

Infodis/TIMC (URA D1618), Institut Albert Bonniot, Faculté de Médecine, F38706, La Tronche CEDEX, France

(*Received* 11 *March* 1993; *accepted* 19 *September* 1994)

Abstract

Ferredoxins (Fd) are electron-carrier proteins, the active sites of which are organized around clusters made of iron and inorganic sulfur. The Fd from *Clostridium acidurici* is 55 amino acids long and contains two [4Fe–4S] clusters. Crystals have been obtained in the space group $P4_32_12$, $a = b = 34.441$ (5), $c = 74.778$ (9) Å. The structure was solved by molecular replacement using the Fd from *Peptostreptcoccus asaccharolyticus* as a search model, these two ferredoxins having 37 residues in common. Refinement using molecular-dynamics techniques was then initiated. Successive rounds of model building and refinement gave a structure that includes 45 water molecules with $R = 15\%$. At this stage, the electron-density map clearly revealed discrepancies in the position of two amino acids in the published primary sequence. Refinement based on these modifications led to $R = 14.3\%$ for 3921 reflections up to 1.8 Å resolution. The geometry of the two clusters has been found to be in good agreement with that previously obtained at a lower resolution. Interactions of polypeptide chain with the [4Fe–4S] clusters, the cluster geometry as well as the hydrogen bonds involving S, Sγ, N and water molecules are reported.

Introduction

Iron–sulfur clusters of the [4Fe–4S] cubane type are found in many proteins and they are involved in the catalysis of a variety of reactions, including redox reactions (Beinert, 1990). This functional diversity of the [4Fe–4S] clusters in proteins suggests that the polypeptide chains play an important role in fine tuning the catalytic properties of these enzymes.

Clostridial ferredoxins are known, by their redox activities, to interact with several well characterized partners (Mortenson & Nachos, 1973), such as hydrogenase, certain nitrogenases (such as *Clostridium pasteurianum*), and pyruvate–ferredoxin oxidoreductase. The molecular details of these interactions are still unknown, but probably depend on some structural specificity. Among the 2[4Fe–4S] ferredoxins, only the crystal structure of the ferredoxin from *Peptostreptococcus asaccharolyticus* (*P. asaccharolyticus*) has been determined with a resolution of 2 Å (Adman, Sieker & Jenson, 1973). Recently, the crystal structure of *Clostridium acidurici* (*C. acidurici*), has been determined at a resolution of 5 Å. We report here the current structural model of this ferredoxin at 1.8 Å resolution.

Materials and methods

(*a*) *X-ray diffraction data*

Precession photos of crystals provided by L. C. Sieker show the same space group and unit-cell parameters as those previously reported (Murthy, Hendrickson, Orme-Johnson, Merritt & Phizackerley, 1988). Diffraction data were obtained from measurements at room temperature on a FAST diffractometer equipped with an area detector. Graphite-monochromatized Cu $K\alpha$ radiation was used. Unit-cell dimensions are $a = b = 34.441$ (5), $c = 74.778$ (9) Å. Systematic extinctions confirm the tetragonal space group $P4_32_12$ or $P4_12_12$ (the former was later shown to be correct). 4500 unique reflections up to 1.8 Å were obtained and 3921 of them had $F_o > 2\sigma$ (*MADNES*, Pflugrath & Messerschmidt, 1988; Collaborative Computational Project, Number 4, 1994).

(*b*) *Structure determination and refinement*

The structure of *C. acidurici* ferredoxin was solved by the molecular-replacement (MR) method (*MERLOT/CCP*4, Fitzgerald, 1988). Atomic coordinates used were from *P. asaccharolyticus*. The *R* factor of the model obtained by MR was 32% for all reflections in the data shell 5–3 Å.

Initially, slow-cooling refinement (*X-PLOR*, Brünger, 1990) using the standard force-field constants tended to distort the Fe—S distances and S—Fe—S angles leading to an unrealistic [4Fe–4S] cluster geometry; as a result this convergence was stopped at a rather high *R* factor of 27%.

In order to prevent over-distortion of the iron–sulfur cluster geometry, a new series of refinements using the

Table 1. *Hydrogen bonding* (Å), *dihedral angles* (°) *in cysteine and covalent bonds in* [Fe–4S] *clusters for C. acidurici*

Hydrogen bonds around cluster I

	N—H···S (Å)	N—H—S (°)		N—H···S (Å)	N—H—S (°)
N9—$S_2$56	3.38	158	N13—Sγ11	3.44	169
N30—Sγ8	3.64	172	N14—$S_4$56	3.57	140
N10—Sγ8	3.39	152	N49—Sγ47	3.55	140
N12—$S_1$56	3.21	153	N51—Sγ47	3.33	167

Hydrogen bonds around cluster II

	N—H···S (Å)	N—H—S (°)		N—H···S (Å)	N—H—S (°)
N38—$S_1$57	3.44	163	N42—Sγ40	3.42	163
N2—Sγ37	3.39	163	N43—$S_3$57	3.40	138
N39—Sγ37	3.52	164	N20—Sγ18	3.64	147
N41—$S_4$57	3.29	156	N22—Sγ18	3.27	163

Fe—S_γ—C_β—C_α dihedral angles (°) in *C. acidurici* involving Fe and cysteine where (Cys_i Fe_j) indicates the S_γ of Cys_i and Fe_j

	Cluster I			Cluster II	
	P. asaccharolyticus	*C. acidurici*		*P. asaccharolyticus*	*C. acidurici*
(Cys_8 Fe_1)	62	61	(Cys_{37} Fe_2)	61	65
(Cys_{47} Fe_4)	86	86	($Cys_{18}Fe_1$)	84	80
(Cys_{14} Fe_3	244	247	(Cys_{43} Fe_4)	252	254
(Cys_{11} Fe_2)	302	301	(Cys_{40} Fe_3)	298	307

S_γ—C_β—C_α—N dihedral angles in cysteine (°)

Cluster I		Cluster II	
(Cys8)	181	(Cys18)	181
(Cys47)	185	(Cys37)	180
(Cys14)	57	(Cys43)	47
(Cys11)	78	(Cys43)	75

Fe—S_γ covalent bond lengths in [4Fe–4S] clusters (Å)

Cluster I		Cluster II	
Fe1—Sγ8	2.309	Fe1—Sγ18	2.288
Fe2—Sγ11	2.315	Fe2—Sγ37	2.322
Fe3—Sγ14	2.304	Fe3—Sγ40	2.309
Fe4—Sγ47	2.282	Fe4—Sγ43	2.289

modified force constants were performed (TranQui *et al.*, 1995). These later refinements led to a reasonable model and decreased the *R* factor down to 23%. At this point the model obtained generated only two short intermolecular contacts of about 2.2 Å solely involving side-chain atoms. It appeared that both short contacts were due to differences in the amino-acid sequences of *P. asaccharolyticus* and *C. acidurici*. Further refinements alternated with difference Fourier maps and graphic aided readjustments (*TOM*, Cambillau, 1989) have slowly reduced the *R* factor to 15% for 3921 reflections up to 1.8 Å. A close inspection of the shape of the electron density (Fig. 1) around the side chain of the Asp15 residue suggested that the 15th residue in the *C. acidurici* sequence was glutamic rather than aspartic acid.

Replacements of Asp15 by Glu15 in the structural model, followed by 12 refinement cycles, reduced the *R* factor to 14.5%. This sequence modification was later confirmed by a resequencing experiment. Furthermore, the resequencing suggested the following additional changes: Asp21→Asn21, Gly25→Ser25, Gly27→Asp27 and Ser28→Asp28. Model rebuilding based on the new sequence and subsequent refinement, however, indicated that the amino-acid sequence around this region is still crystallographically uncertain. After introduction of 45 water molecules and replacement of Asp15 by Glu 15, a new difference Fourier map showed electron density around the (res25-res26-res27-res28) region at the 1.2σ contour level allowing the localization of the (res25-res26-res27-res28) loop. The electron-density shape for the (res25-res26-res27-res28) region was, however, still broad even after subsequent refinements, compared to other regions of the molecule. Finally, refinements including both [4Fe–4S] clusters, 447 protein atoms and 45 water molecules reduced the *R* factor to 14.3% for reflections in the range of 5–1.3 Å (15.7% for all reflections) and led to a model with reasonable φ and ψ angles (Ramakrishnan & Ramachandran, 1965) (Fig. 2). The norms and r.m.s. values of temperature factors for cluster atoms, main chain, side chains and water molcules are (7.11, 0.88 $Å^2$), (11.3, 4.5 $Å^2$), (17.4, 9.0 $Å^2$), and (30.3, 11.9 $Å^2$), respectively.*

The r.m.s. deviations from the ideal bond lengths for main chain, side chains, clusters and water molecules are 0.012, 0.012, 0.017 and 0.023 Å, respectively.

Results and discussion

As expected, the general folding, [4Fe–4S]-cluster positions and arrangements of both *C. acidurici* and *P. asaccharolyticus* exhibit similar features: (*a*) [4Fe–4S]

* Norm $= (\sum x_i^2/n)^{1/2}$, r.m.s. $= [\sum (x_i - \langle x \rangle)^2/n]^{1/2}$.

clusters are separated by 12.0 Å and are buried inside the polypeptide chain conferring to the *C. acidurici* molecule an ellipsoid shape with an approximate dimension of $26 \times 26 \times 28$ Å; (*b*) the coordination of cysteine is preserved; (*c*) hydrophobic residues tend to pack around the iron–sulfur cluster in such a way that almost all of the [4Fe–4S] faces are screened from direct interaction with solvent molecules by proper orientations of the surrounding hydrophobic side chains. Thus, it is observed that the spatial arrangements of tyrosine rings (Tyr2 and Tyr29 for clusters I and II, respectively) tend to prevent direct contact between cluster and solvent. A similar arrangement has been found in *P. asaccharolyticus* (Adman, Watenpaugh & Jensen, 1975).

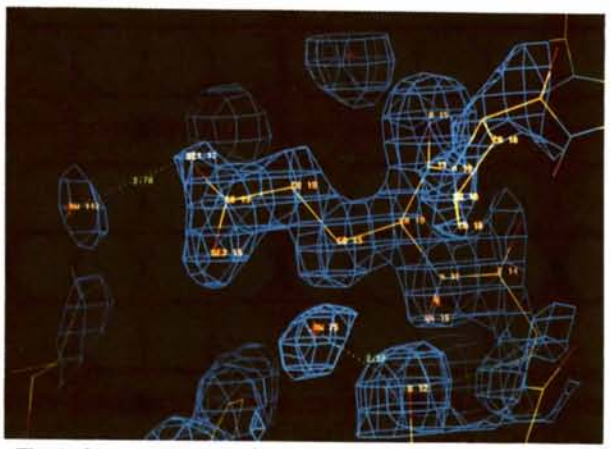

Fig. 1. Observed ($2F_o - F_c$) electron density of Glu15 side chain.

(*a*) *Geometry and environment of* [4Fe–4S] *clusters*

The geometry of the iron–sulfur cluster is cubane-like; each Fe atom is linked to three S atoms and each S atom has three Fe atoms as immediate neighbours (Fig. 3). The average Fe—S bond length, 2.31 Å, in both [4Fe–4S] clusters is of the same order as that observed in *P. asaccharolyticus* (2.31 Å).

As in the *P. asaccharolyticus* protein, each of the two [4Fe–4S] clusters in *C. acidurici* are attached to the protein chain by four covalent Fe—S_γ bonds at Cys8, Cys11, Cys14, Cys47 for cluster I and Cys18, Cys37, Cys40, Cys43 for cluster II. The Fe—S_γ bond lengths ranging from 2.28 to 2.34 Å, suggest that they are covalent–preponderant in character.

In addition to the links of each [4Fe–4S] to the polypeptide chain by the four Fe–S_γ bonds, N—H···S hydrogen bonds enhance the stability of the [4Fe–4S] positions relative to their immediate hydrophobic neighbours by anchoring the amide groups in the vicinity of the inorganic cluster. The hydrogen-bond network involving the cluster and nearby amide groups in *C. acidurici* and in *P. asaccharolyticus* are compared

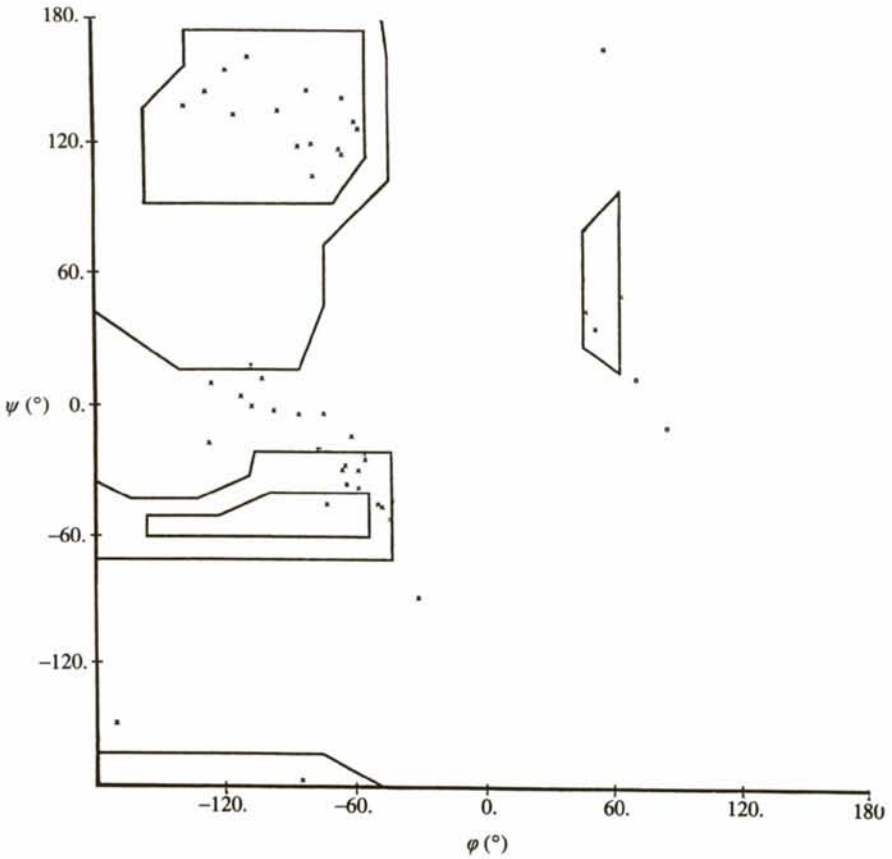

Fig. 2. Ramachandran plot of the main-chain dihedral angles.

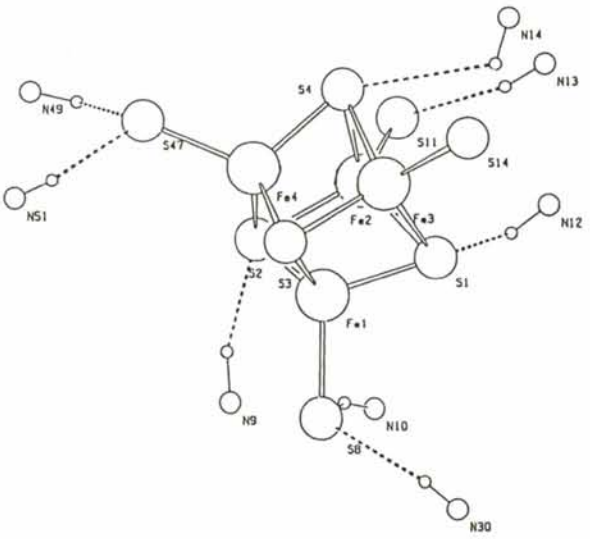

Cluster I

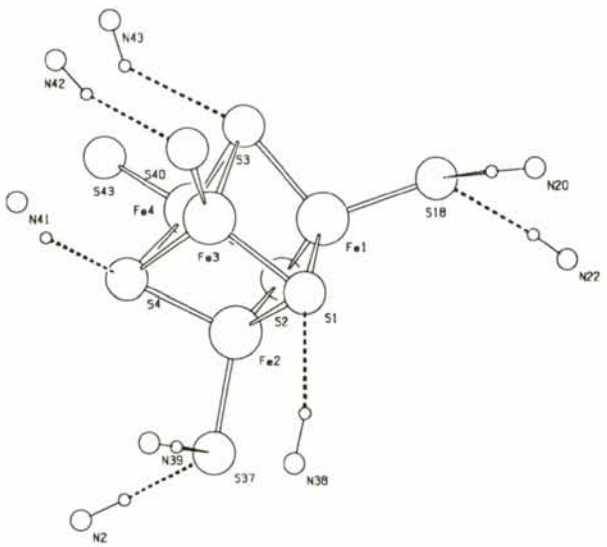

Cluster II

Fig. 3. [4Fe–4S] clusters I and II and their immediate environment and associated hydrogen bonds.

in Table 1. Again, the immediate environment of the [4Fe–4S] cluster is preserved in *C. acidurici* and in *P. asaccharolyticus* (Adman, Watenpaugh & Jensen, 1975). Moreover, it is worth noting that the tyrosine rings (Tyr2 and Tyr29 for cluster I and II, respectively) protect clusters from direct contact with solvent molecules; these interactions are similar in *C. acidurici* and the [4Fe–4S] *P. asaccharolyticus* species (Fig. 4).

(*b*) *Folding of the polypeptide chain*

As mentioned above, the conformation of the polypeptide chain in *C. acidurici* is mainly governed by the bonding requirements involved in joining eight cysteine groups with two [4Fe–4S] clusters through Fe—S_γ covalent bonds. Therefore, it is to be expected that the organization of the polypeptide chain around the [Fe—4S] cluster will remain similar in *P. asaccharolyticus* and in *C. acidurici*. To some extent, this similarity spreads over the whole molecule with only one exception for the inserted region defined by the (res25-res26-res27-res28) loop. The relatively high atomic thermal factors associated with this region (characterized by rather ill defined electron density) suggest that the (res25-res26-res27-res28) segment is subjected to static and/or dynamic conformational disorder.

This assumption is supported by the fact that this region, located on the surface of the protein, far from the [4Fe–4S] centers, may by exposed to solvent interactions. Furthermore, this loop is also located in the longest stretch of chain that contains no strict homology to any of the other ferredoxins, implying that it has sufficient flexibility to accommodate amino-acid changes without affecting the integrity of the molcule. Similar disorder has been recently observed in the one-[4Fe–4S] cluster ferredoxins of *B. thermoproteolyticus* (residues 28–30); this area in the crystal structure has large temperature factors and the weakest electron density (Fukuyama, Matsubara, Tsukihara & Katsube, 1989). It is not unreasonable to expect that a similar phenomenon occurs in *C. acidurici*. The atomic coordinates in this disordered region are very approximate.

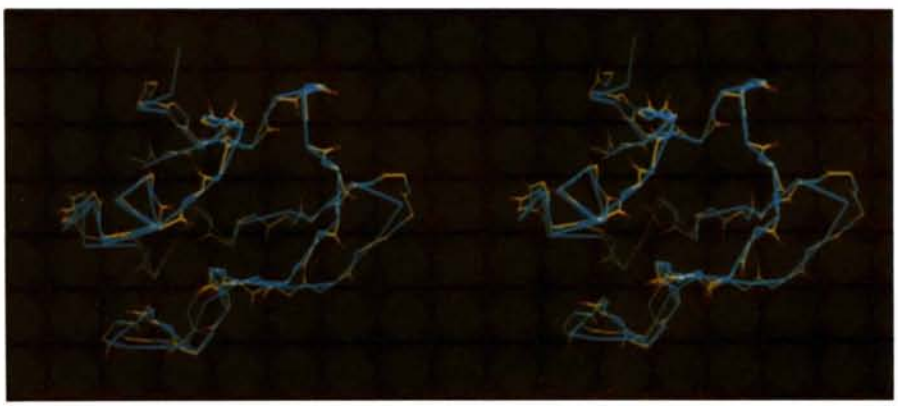

Fig. 4. Superposition of glycine and tyrosine rings in the vicinity of [4Fe–4S] clusters in *C. acidurici* and *P. asaccharolyticus* (For clarity only Tyr and Gly of *P. asaccharolyticus* are represented.)

Table 2. *Water molecules and hydrogen bonds*

Water molecules ligated to protein through strong hydrogen bonds

Residue	Water	Distance (Å)	Residue	Water	Distance (Å)
Tyr2/OH	Ow2	2.67	Tyr2/O	Ow4	2.74
Ala7/O	Ow1	2.74	Ser10/O	Ow19	2.86
Gly12/O	Ow5	2.73	Glu15/O	Ow6	2.87
Val20/O	Ow37	2.85	Ser24/OG	Ow14	2.89
Gln25/OE1	Ow19	2.80	Gly26/O	Ow32	2.82
Gly27/O	Ow11	2.71	Tyr30/O	Ow2	2.84
Asp33/OD2	Ow41	2.87	Asp33/OD2	Ow45	2.84
Ala34/O	Ow17	2.76	Thr36/O	Ow7	2.74
Cys37/O	Ow17	2.71	Ile38/O	Ow13	2.83
Cys40/O	Ow23	2.86	Gly41/O	Ow20	2.76
Ala42/O	Ow22	2.87	Ala44/O	Ow24	2.73
Val46/O	Ow9	2.76	Pro48/O	Ow42	2.75
Pro52/O	Ow10	2.79	Ala55/OT2	Ow10	2.78

Water molecules ligated to other water molecules

Water	Water	Distance (Å)	Water	Water	Distance (Å)
Ow2	Ow1	2.85	Ow11	Ow26	2.77
Ow14	Ow34	2.84	Ow14	Ow38	2.85
Ow18	Ow4	2.79	Ow38	Ow41	2.78
Ow33	Ow34	2.81	Ow40	Ow44	2.80

Structural data at low temperatures and inelastic neutron-scattering spectroscopy would be useful to separate the dynamic and static contributions, hence providing more insight on the temperature dependence of dynamics in *C. acidurici*.

(*c*) *Water molecules, hydrogen bonds and crystal packing*

45 water molecules have been unambiguously localized by difference-Fourier peaks. Others, corresponding to ill defined electron density, may be ascribed to more loosely linked waters. They are not included in Table 2, even though their contribution, mediated by hydrogen bonds, as a packing force may be crucial for crystal cohesion. No evidence of other solvent species (*e.g.* ammonium sulfate which was used in crystal growth) has been found. The distribution of water molecules around the ferredoxin molecule is shown in Fig. 5. Water molecules are mostly distributed outside and near the surface of the protein molecule. Some water molecules, however, are deeply buried inside the molecule and serve to establish strong hydrogen bonds between adjacent peptide chains.

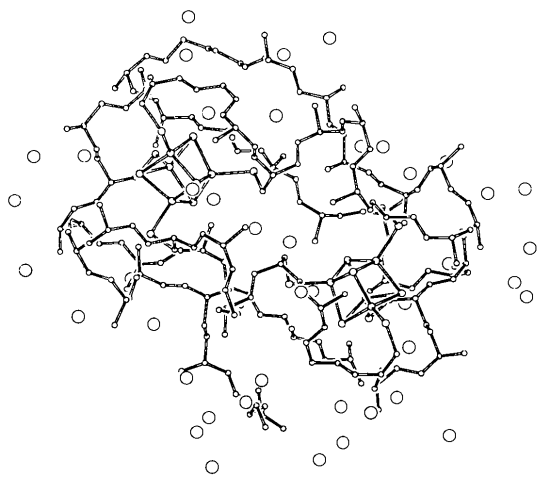

Fig. 5. Distribution of water molecules around the *C. acidurici* protein: most water molecules are located near the surface (drawn with *PLUTON*, Spek, 1992).

Localized water molecules seem to play two different roles: (*a*) those near the surface are hydrogen bonded preferentially to polar groups on the protein, and (*b*) those that establish contacts between two symmetrically related molecules.

Concluding remarks

The high-resolution data (1.8 Å) used to determine and to refine the *C. acidurici* structure give, in addition to the confirmation of the similarity between the *P. asaccharolyticus* and *C. acidurici* species, (*a*) a better definition of the positions of the Cα chain and associated side chains, (*b*) a correction of the sequence error and (*c*) the localization of the inserted region (residues 25–28). They also give a more accurate description of the [4Fe–4S] cluster geometry, information that is essential for an understanding of the redox activity in this class of proteins.*

The authors would like to thank Dr L. C. Sieker for growing the crystals.

* Atomic coordinates and structure factors have been deposited with the Protein Data Bank, Brookhaven National Laboratory. Free copies may be obtained through The Managing Editor, International Union of Crystallography, 5 Abbey Square, Chester CH1 2HU, England (Reference: GR0252). A list of deposited data is given at the end of this issue.

References

ADMAN, E. T., SIEKER, L. C. & JENSEN, L. H. (1973). *J. Biol. Chem.* **248**, 3987–3996.

ADMAN, E. T., WATENPAUGH, K. D. & JENSEN, L. H. (1975). *Proc. Natl Acad. Sci. USA.* **72**, 4854–4858.

BEINERT, H. (1990). *FASEB J.* **4**, 2483–2491.

BRÜNGER, A. (1990). *X-PLOR Manual.* Version 1.5. Department of Biophysics, Yale Univ., Newhaven, CT 06511, USA.

CAMBILLAU, C. M. (1989). *TOM. Molecular Graphics Program.* LCCMB Faculté de Médicine Nord, Marseille, France.

COLLABORATIVE COMPUTATIONAL PROJECT, NUMBER 4 (1994). *Acta Cryst.* **D50**, 760–763.

FITZGERALD, P. M. D. (1988). *J. Appl. Cryst.* **21**, 273–278.

FUKUYAMA, K., MATSUBARA, H., TSUKIHARA, T. & KATSUBE, Y. (1989). *J. Mol. Biol.* **210**, 383–398.

MORTENSON, L. E. & NACHOS, J. (1973). In *Iron-Sulfur Proteins*, Vol. 1, edited by W. LOVENBERG, pp. 37–64. New York: Academic Press.

MURTHY, H. M. K., HENDRICKSON, W. A., ORME-JOHNSON, W. H., MERRITT, E. & PHIZACKERLEY, R. P. (1988). *J. Biol. Chem.* **263**, 18430–18436.

PFLUGRATH, J. W. & MESSERSCHMIDT, A. (1988). *MADNES User's Guide.* Max Planck Institute, Munich, Germany.

RAMAKRISHNAN, C. & RAMACHANDRAN, G. N. (1965). *Biophys. J.* **5**, 909–933.

SPEK, A. L. (1992). *PLUTON.* Bijovet Center for Biomolecular Research, Utrecht, The Netherlands.

TRANQUI, D., HERMOSO, J. A., AVERBUCH, M. T., TAMAGNAN, G., LECLERC, G. & CUSSAC, M. (1995). *Acta Cryst.* B**51**, 96–80.